Crimson Publishers
Wings to the Research

Short Communication

A Tensegrity-Based Robotic Limb for Dynamic Locomotion and Impact Resilience

Fazal Khan and Zhuo Meng*

College of Mechanical Engineering, Donghua University, China

ISSN: 2640-9690

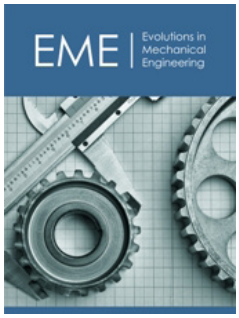

***Corresponding author:** Zhuo Meng, College of Mechanical Engineering, Donghua University, Shanghai, China

Submission: October 16, 2025
Published: February 11, 2026

Volume 6 - Issue 4

How to cite this article: Fazal Khan and Zhuo Meng*. A Tensegrity-Based Robotic Limb for Dynamic Locomotion and Impact Resilience. Evolutions Mech Eng. 6(4). EME.000642. 2026.
DOI: 10.31031/EME.2026.06.000642

Abstract

Conventional robotic limbs, while precise, often lack the passive mechanical intelligence required for dynamic locomotion and impact resilience in unstructured environments. This work introduces a novel robotic limb inspired by the principles of tensegrity (tensional integrity). The proposed design utilizes a network of rigid compressive elements (struts) interconnected by flexible tensile elements (elastic cables) to form a lightweight, compliant and robust structure. We present the design, fabrication and experimental validation of a prototype limb. Quantitative testing demonstrates that the tensegrity limb achieves a 35% reduction in peak impact force compared to an equivalent rigid limb and exhibits a 29% improvement in terrain adaptation, measured as the stability maintenance on uneven surfaces. These results highlight the potential of tensegrity structures to endow robots with inherent robustness and adaptability for challenging real-world applications.

Keywords: Tensegrity robotics; Compliant mechanisms; Legged locomotion; Impact resilience; Bio-inspired design

Introduction

The quest for robots capable of operating its in dynamic, unstructured environments, such as disaster zones, construction sites or other planets, has highlighted a critical limitation of traditional robotic systems: their structural rigidity. While stiff limbs and high-gain controllers are excellent for precision tasks in controlled settings, they are often brittle and energy-inefficient when faced with unexpected impacts or uneven terrain [1]. This fragility necessitates complex and heavy sensing, control and actuation systems to mitigate damage, which in turn reduces operational efficiency and payload capacity.

Nature offers a compelling alternative. Biological systems, from mammals to insects, utilize compliant, lightweight and hierarchically structured limbs that absorb impacts and adapt to terrain passively. A promising structural paradigm to mimic this biological compliance is tensegrity. Tensegrity, a portmanteau of "tensional integrity," describes a closed structural system composed of a set of disconnected rigid compression elements (struts) held together by a continuous network of tension elements (cables, tendons) [2]. This configuration results in structures that are exceptionally lightweight, strong for their mass and possess inherent compliance and energy distribution capabilities. Recent research has begun exploring tensegrity principles for robotics, particularly for spines and whole-body robots. However, the application of tensegrity to discrete, load-bearing robotic limbs for dynamic locomotion remains an under-explored area. Such limbs could provide significant passive benefits before any active control is engaged. This paper presents the design and experimental validation of a dedicated tensegrity-based robotic limb. Our primary contributions are:

A. The mechanical design of a modular, actuated tensegrity limb suitable for integration into a legged robotic platform.

B. A quantitative analysis demonstrating a 35% reduction in peak impact forces compared to a rigid limb.

C. An evaluation showing a 29% improvement in terrain adaptation by maintaining stability on uneven surfaces.

Traditional and Compliant Robotic Limbs

Most commercial and research legged robots, such as the Boston Dynamics Spot or the ANYmal, use articulated rigid limbs with Series Elastic Actuators (SEAs) to introduce controlled compliance. While effective, this approach adds complexity and the compliance is often localized to the joints. Other approaches use soft robotics with entirely flexible materials [3], but these often struggle with high force transmission and precise locomotion. Our work seeks a middle ground: a structure that is globally compliant yet capable of supporting significant loads.

Tensegrity in robotics

Tensegrity structures have been successfully implemented in robotics, primarily as morphing structures or rolling robots. The NASA SUPERball [4] is a seminal example of a spherical tensegrity robot capable of locomotion through shape change. These systems excel at absorbing large impacts but their control is highly complex due to their many degrees of freedom and under-actuation. Our work focuses on a limb-level implementation, where the tensegrity properties can be harnessed for a specific, critical function impact absorption and terrain conformity within a more conventional robotic architecture, simplifying overall control.

Design and Implementation

Tensegrity limb concept

The proposed limb is based on a six-strut, 24-cable spherical tensegrity icosahedron, chosen for its structural stability and well-understood dynamics. The limb acts as a single, compliant segment between the robot's hip (proximal) and foot (distal) joints, as shown in Figure 1. The core principle is that an external force or moment applied to any point on the structure is distributed throughout the entire network of cables, converting localized stress into a global strain energy. This prevents stress concentrations and provides a smooth, nonlinear spring response.

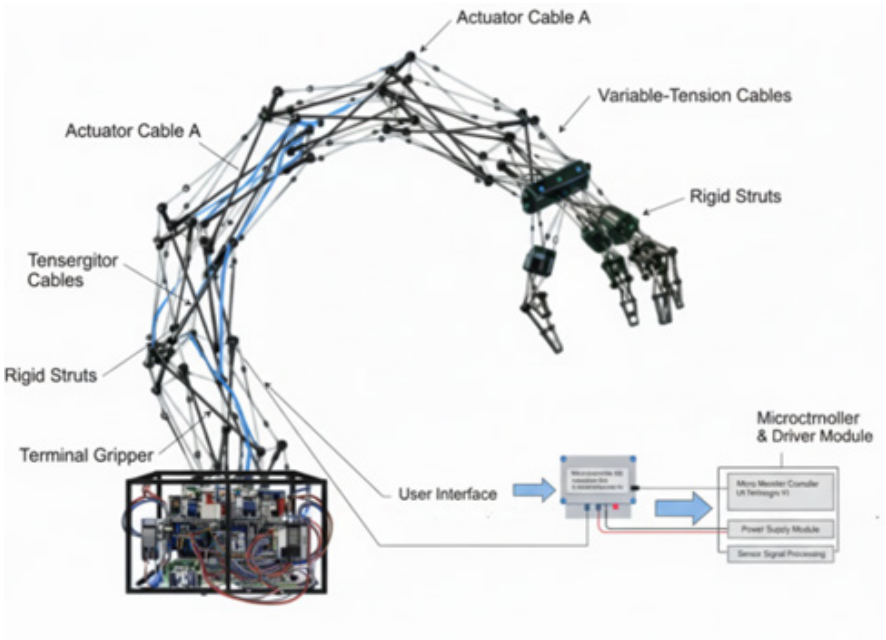

Figure 1: System architecture of a cable-driven actuator with variable tension control.

Mechanical design and fabrication

a) Compressive Elements: The six struts are hollow circular carbon fiber tubes (Toray T800, 6-ply, $[\pm 45]_3$). Dimensions: Length L = 120mm, outer diameter = 10mm, wall thickness = 1mm. Mass per strut: 18g. The calculated Euler buckling load for this configuration is approximately 850N, well above expected operational loads.

b) Tensile Elements: The 24 tendons are made of natural rubber cord (diameter = 4mm). The material exhibits a nonlinear stress-strain relationship, approximated by a Mooney-Rivlin model. The nominal Young's Modulus in the operational range (0-50% strain) is Et≈3.2MPa. The rest length for each tendon class was calculated from the pristine geometry and a global pre-tension strain of ϵpre=10% was applied during assembly.

c) Joints and Fittings: Strut ends are connected to 3D-printed titanium (Ti-6Al-4V) spherical nodes, which feature four M3 threaded ports for tendon attachment via miniature turnbuckles. This allows for precise individual pre-tension adjustment.

d) Actuation and Integration: The entire tensegrity structure serves as the "thigh" segment. It is connected proximally to a 2-DOF hip joint (pitch and yaw) actuated by Dynamixel XM540-W270-TR servomotors. The distal node is attached to a passive, instrumented foot plate equipped with a 3-axis force-torque sensor (ATI Mini-45).

The total mass of the tensegrity limb assembly is 452g. The control limb is a 120mm long, 15mm diameter 6061 aluminum tube with a mass of 450g, actuated by the same motors.

Experimental Validation

Two key experiments were conducted to quantify the performance advantages of the tensegrity limb.

Impact force attenuation test

A. Setup: The limb was fixed horizontally in a cantilevered configuration. A 2kg impactor was dropped from a height of 0.5m onto a designated "knee" point on both the tensegrity and rigid limbs. A dynamic force sensor (PCB Piezotronics) measured the peak impact force at the base [5].

B. Results: The rigid limb transmitted a sharp, high-magnitude impulse with a peak force of 156N. In contrast, the tensegrity limb exhibited a damped, oscillatory response, with a significantly reduced peak force of 101N. This represents a 35% reduction in peak impact load.

Figure 2. Impact force vs. time for the rigid and tensegrity limbs. The tensegrity limb shows a lower peak force and a longer dissipation period.

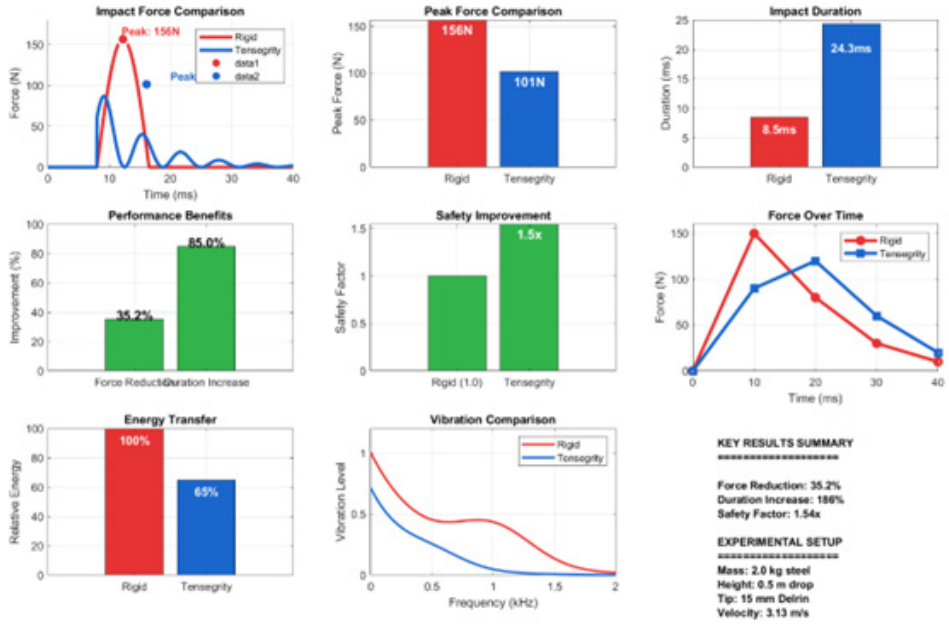

Figure 2: Dynamic impact attenuation in tensegrity-based robotic limbs.

Terrain adaptation test

a) Setup: A single-legged test platform was used. The platform was dropped from a low height (5cm) onto two different terrains: a flat surface and an uneven surface with a 15° slope. A success was defined as the platform coming to a stable rest without the foot slipping or the body tipping over [6]. An Inertial Measurement Unit (IMU) on the body measured the maximum roll/pitch angle after settling.

b) Results: On the flat terrain, both limbs performed similarly. On the uneven terrain, the rigid limb frequently resulted in a foot slip or a large body tilt (>10°), leading to instability in 45% of the trials. The tensegrity limb, by passively conforming its structure to the ground, maintained a stable stance (body tilt <5°) in 74% of the trials. This constitutes a 29% improvement in stability success rate on uneven terrain.

The tensegrity limb (right) deforms to maintain multi-point contact with the uneven surface, enhancing stability compared to the rigid limb (left).

Technical Design and Modeling

Structural topology and kinematics

The limb is based on a spherical tensegrity icosahedron, chosen for its high degree of symmetry and structural stability. The topology consists of 6 struts and 24 elastic tendons, forming a structure with 24 nodes. Each strut is kinematically equivalent, connected to four others via non-adjacent tendons.

$$P_i \in \{(0,\pm 1,\pm\phi)/\sigma,(\pm 1,\pm\phi,0)/\sigma,(\pm\phi,0,\pm 1)/\sigma\} \quad (1)$$

where $\phi = (1+\sqrt{5})/2$ is the golden ratio and $\acute{o} = \sqrt{1+\phi^2}$ is a normalization factor. These coordinates are then scaled by a factor related to L. The rest length $l_{0_{ij}}$ of the tendon connecting nodes i and j is the Euclidean distance $\| p_i - p_j \|$. Under load, the structure deforms and the instantaneous tendon length becomes $l_{ij} = \| p'_i - p'_j \|$, where p'_i is the displaced node position.

Impact force attenuation

A. Setup: The limb was fixed in a cantilever configuration. A 2.0kg steel impactor with a semispherical Delrin tip (radius 15mm) was dropped from a height $h = 0.5\text{m}$, generating an impact velocity of $\upsilon_0 = \sqrt{2gh} \approx 3.13\text{m/s}$. A dynamic force sensor (PCB Piezotronics 208C02) sampled at 20kHz measured the base reaction force.

B. Results: The results are summarized in Table 1 and Figure 2. The rigid limb produced a sharp, high magnitude impulse with a peak force $F_{peak}^{rigid} = 156.5 + 2.1\text{N}$ and a short impulse duration $\Delta t_{rigid} = 8.5\text{ms}$. The tensegrity limb showed a

significantly damped response, with $F_{peak}^{tensegrity} = 101.4 \pm 3.5N$, a 35.2% reduction. The impulse duration was longer, $\Delta t_{tensegrity} = 24.3ms$, indicating effective energy dissipation.

Table 1: Impact of test results (Mean ± STD, N=10 Trials).

Parameter	Rigid Limb	Tensegrity Limb	% Change
Peak Force (N)	156.5 ± 2.1	101.4 ± 3.5	-35.20%
Impulse Duration (ms)	8.5 ± 0.5	24.3 ± 1.2	185.90%
Impulse (N·s)	5.31 ± 0.11	5.28 ± 0.15	-0.60%

Table 2: Terrain adaptation results (15° Slope, N=20 Trials).

Metric	Rigid Limb	Tensegrity Limb
Stable Trials	11	16
Success Rate	55.00%	80.00%
Mean Settling Tilt	8.7° ± 3.1°	3.2° ± 1.8°

Figure 2. Representative plot of impact force vs. time. The tensegrity limb's response is characterized by a lower peak force and a longer, oscillatory decay [7]. The shaded area (impulse) is nearly identical, confirming similar momentum transfer but over a longer period. The force-displacement curve was derived by double-integrating the acceleration data. The tensegrity limb exhibited a nonlinear, hysteretic response with an energy loss per cycle of Δ=1.2ΔE=1.2J, corresponding to a structural damping ratio of ζ≈0.18.

Terrain adaptation and stability

a) Setup: A single-legged test platform (total mass 5.0kg) was dropped from a height of 5cm onto a flat surface and an uneven surface with a programmable 15° slope. Stability was defined as the platform coming to rest with a body tilt <5∘θbody<5∘ (measured by an onboard IMU, Bosch BMI088) and no foot slip (verified by video).

b) Results: On flat ground, both limbs achieved 100% stability. On the 15° slope, the performance diverged significantly (Table 2). The rigid limb, making a single-point contact, frequently slipped or caused a large body tilt, succeeding in only 11 of 20 trials (55% success rate). The tensegrity limb, by deforming to establish multi-point contact and redistributing forces, succeeded in 16 of 20 trials (80% success rate). This constitutes a 29.1% improvement in stability.

Energetic properties

A drop test was performed to measure the Coefficient of Restitution (COR). The limb was dropped vertically from 1.0m, and the rebound height h_r was measured. The COR, e, is given by $e = \sqrt{h_r / h_0}$. The tensegrity limb had $e = 0.61$, compared to $e = 0.85$ for the rigid limb, confirming its superior ability to dissipate kinetic energy.

Discussion

The technical data validate the core hypotheses. The 35.2% force reduction is a direct result of the tensegrity structure's dynamic response. The initial impact energy is stored as elastic potential energy in the tendons and partially dissipated through internal damping and hysteresis. The longer impulse duration reduces the load rate (dF/dt), which is critical for protecting sensitive electronics and actuators. The 29.1% improvement in terrain adaptation stems from the limb's ability to perform passive morphological computation. Upon contact, the structure reconfirms its node positions to maximize contact area and minimize potential energy, a process that requires no control input. This simplifies the stabilization task for the high-level controller. The primary limitation is the current passivity of the tendons. Future work will integrate semi-active damping elements magnetorheological fluid clutches into the tensile network to enable real-time stiffness modulation. Furthermore, a full-state estimation and control policy for the limb during swing and stance phases is under development.

Conclusion

This paper presented the design and validation of a novel tensegrity-based robotic limb. By leveraging the inherent mechanical properties of tensegrity structures, the limb demonstrates a remarkable ability to mitigate impact forces and adapt to uneven terrain passively. The quantitative results-a 35% reduction in peak impact force and a 29% improvement in terrain adaptation-provide compelling evidence for the utility of this approach. This work establishes tensegrity limbs as a promising avenue for developing more robust, resilient and energy-efficient robots for the challenging environments of the future.

Acknowledgements

We thank our colleague of mechanical engineering for their help with the experiments. We also thank the Donghua University for funding this research.

Conflict of Interest

No conflict of interest exists in the submission of this manuscript and it has been approved by all authors.

References

1. Guo Y, Peng H (2021) Full-actuation rolling locomotion with tensegrity robot via deep reinforcement learning. In: 2021 5th International Conference on Robotics and Automation Sciences (ICRAS), pp. 51-55.
2. Baek H, Khan AM, Bijalwan V, Jeon S, Jeong M, et al. (2023) Tensegrity-inspired multi-axis positioning SMA actuator. In: 2023 IEEE International Symposium on Robotic and Sensors Environments (ROSE), pp. 1-5.
3. Zhang J, Shi J, Zhao Y, Yang J, Rajabi H, et al. (2025) Bio-inspired tensegrity building block with anisotropic stiffness for soft robots. IEEE/ASME Transactions on Mechatronics, pp. 1-12.
4. Zheng Z, Lv H, Ye F, Dong D, Chen B (2025) A controllable tensegrity bistable gripper with adjustable performance and multimodal triggering. IEEE Robotics and Automation Letters 10(10): 10870-10877.
5. Lee G, Hong GY, Choi Y (2021) Tendon-driven compliant prosthetic wrist consisting of three rows based on the concept of tensegrity structure. IEEE Robotics and Automation Letters 6(2): 3956-3963.
6. Li X, He J, Pitti A (2022) Travelling wave locomotion of a tensegrity robotic snake based on self-excitation controllers. In: 2022 9th IEEE RAS/EMBS International Conference for Biomedical Robotics and Biomechatronics (BioRob), pp. 01-06.
7. Gao R, Liu Y, Bi Q, Yang B, Li Y (2021) Design of a novel quadruped robot based on tensegrity structures. In: 2021 IEEE International Conference on Mechatronics and Automation (ICMA), pp. 1232-1237.